

The DARC site: a database of aligned ribosomal complexes

Alexander Jarasch^{1,2}, Philipp Dziuk¹, Thomas Becker¹, Jean-Paul Armache¹,
Andreas Hauser¹, Daniel N. Wilson^{1,2,*} and Roland Beckmann^{1,2,*}

¹Gene Center and Department for Biochemistry and ²Center for integrated Protein Science Munich (CiPSM), University of Munich, Feodor-Lynenstr. 25, 81377 Munich, Germany

Received August 12, 2011; Accepted September 18, 2011

ABSTRACT

The ribosome is a highly dynamic machine responsible for protein synthesis within the cell. Cryo-electron microscopy (cryo-EM) and X-ray crystallography structures of ribosomal particles, alone and in complex with diverse ligands (protein factors, RNAs and small molecules), have revealed the dynamic nature of the ribosome and provided much needed insight into translation and its regulation. In the past years, there has been exponential growth in the deposition of cryo-EM maps into the Electron Microscopy Data Bank (EMDB) as well as atomic structures into the Protein Data Bank (PDB). Unfortunately, the deposited ribosomal particles usually have distinct orientations with respect to one another, which complicate the comparison of the available structures. To simplify this, we have developed a *Database of Aligned Ribosomal Complexes*, the DARC site (<http://darcsite.genzentrum.lmu.de/darc/>), which houses the available cryo-EM maps and atomic coordinates of ribosomal particles from the EMDB and PDB aligned within a common coordinate system. An easy-to-use, searchable interface allows users to access and download >130 cryo-EM maps and >300 atomic models in the format of brix and pdb files, respectively. The aligned coordinate system substantially simplifies direct visualization of conformational changes in the ribosome, such as subunit rotation and head-swiveling, as well as direct comparison of bound ligands, such as antibiotics or translation factors.

INTRODUCTION

The past 10 years have seen a dramatic increase in the number of structures of ribosomal particles determined by cryo-electron microscopy (cryo-EM) and X-ray crystallography. From a crystallographic viewpoint, structures of ribosomal particles are now available from three different bacterial organisms [*Escherichia coli* 70S (1), *Thermus thermophilus* 30S (2,3) and 70S (4,5), as well as *Deinococcus radiodurans* 50S (6)], one archaeon [*Haloarcula marismortui* 50S] and two eukaryotes [*Tetrahymena thermophila* 40S (7) and *Saccharomyces cerevisiae* 80S (8)]. Similarly, cryo-EM has been used to determine structures of a wide-range of bacterial ribosomes, predominantly from *E. coli* (9), but also *T. thermophilus* (10), organellar ribosomes [Spinach chloroplast 70S (11) and mammalian mitochondrial 55S (12)] as well as cytoplasmic ribosomes from both higher eukaryotes, including mammals [e.g. human 40S (13), rat 80S (14), rabbit 80S (15) and canine 80S (16)] and plants [*Triticum aestivum* 80S (17)], and lower eukaryotes, such as yeast (18) and other fungi (19). To date, there are approximately 130 cryo-EM maps of ribosomal particles deposited in the electron microscopy data bank (EMDB; <http://www.ebi.ac.uk/pdbe/emdb/>) and more than 300 pdb entries for atomic coordinates and models of ribosomal particles deposited in the Protein Data bank (PDB; <http://www.pdb.org/pdb>). Their deposition has followed the rapid exponential increase in the overall number of cryo-EM maps and models deposited in the EMDB and PDB, respectively (20,21). Indeed, the new EMDataBank (<http://EMDataBank.org>) has already more than 100 entries for EMDB maps of ribosomal particles linked with associated PDB models (21).

Both cryo-EM and X-ray crystallography have been successfully utilized to determine structures of ribosomal

*To whom correspondence should be addressed. Tel: +49 0 89 2180 76902; Fax: +49 0 89 2180 76999; Email: Wilson@lmb.uni-muenchen.de
Correspondence may also be addressed to Roland Beckmann. Tel: +49 0 89 2180 76900; Fax: +49 0 89 2180 76945;
Email: Beckmann@lmb.uni-muenchen.de

The authors wish it to be known that, in their opinion, the first two authors should be regarded as joint First Authors.

particles in complex with various ligands, ranging from mRNA and tRNA substrates to protein factors and antibiotics [reviewed by (22)]. At the time of writing, approximately 70 cryo-EM maps of ribosomes in complex with tRNAs and ~100 in complex with translation factors were deposited in the EMDB, whereas the PDB contained more than 100 atomic coordinates of ribosomal particles associated with tRNAs, approximately 150 with antibiotics and approximately 100 with protein factors (or domains thereof). The huge wealth of structural information available provides insight into ribosome function by enabling multiple different types of comparisons to be made, for example, between (i) ribosomes of different kingdoms, which provides evolutionary insight into the conserved and kingdom-specific regions of the ribosomes (23,24), (ii) different conformational states of the same ribosomal particle, which can indicate conformational dynamics, for example, the rotational movement of the small subunit with respect to the large subunit (18,25,26), (iii) ribosomes of different species interacting with the same ligand, which is particularly relevant when comparing the binding of antibiotics to antibiotic-susceptible bacteria or resistant archaea (27), (iv) different but closely related ligands bound to the same ribosomal particle, which is exemplified by the plethora of substrate and intermediate mimics used to decipher the mechanism of peptide-bond formation (28), (v) different functional states of the ribosome with the same ligand bound, such as the differing degrees of subunit rotation, head swiveling and L1 stalk movement seen when comparing tRNAs in pre-, intermediate or post-translocational states ribosomes (29,30) and (vi) different functional states of the ribosome induced upon ligand binding, for example subunit rotation upon EF-G binding (25) or remodeling of the small subunit upon HCV IRES binding (13).

However, because the maps and atomic structures deposited in the EMDB and PDB have no common coordinate system, it is usually necessary for the researcher to realign the maps and models of interest to one another. Unfortunately, for the non-expert, this is not always trivial, particular when working with EM density maps. Therefore, we have developed a Database of Aligned Ribosomal Complexes, the DARC site, where users can freely access and download aligned PDBs and cryo-EM density maps. Thus, the downloaded pdb and map (brix) files can be opened in common and freely available viewing programs, such as PyMol (www.pymol.org), Chimera (31), VMD (32) and directly compared.

RESULTS

Database content

The DARC site continuously monitors the release of new structures into the public domain by the EMDB and PDB and imports maps and pdbs of entries that contain ribosomes or ribosomal subunits. Currently, this encompasses cryo-EM maps of bacterial 30S, 50S or 70S particles, archaeal 50S subunits, organellar 70S as well as eukaryotic 40S, 60S and 80S particles. The DARC site does not yet include cryo-EM maps of bacterial or eukaryotic assembly

intermediates. The DARC site comprises atomic coordinates from the PDB related to crystal structures of the bacterial 30S, 50S and 70S, the archaeal 50S and eukaryotic 40S and 80S. In addition, the DARC site contains atomic coordinates for ribosomal structures built into cryo-EM maps, however, does not include all structures of fragments of ribosomal RNA alone or in complex with ligands due to ambiguity with alignment. Similarly, the DARC site does not include some incomplete models that contain only partial fragments of the small or large subunit rRNAs, but does however include atomic coordinates with chains containing only backbone atoms, such as phosphates for rRNA or C α for ribosomal proteins.

Structural alignments

The DARC site uses a common coordinate system based on the cryo-EM maps (EMDB-1067) and associated molecular models (40S, PDB-1S1H and 60S, PDB-1S1I) of the yeast 80S ribosome (18). Cryo-EM maps of ribosomal particles were parsed from the EMDB and the pixel and box size was adjusted to the reference map using SPIDER (33). The readjusted maps were then manually aligned to the EMDB-1067 reference map in Chimera (31). Subsequently an automatic fitting algorithm (fit-in-map) was applied that maximized the cross-correlation coefficient between the parsed and reference maps using a series of alternating rotation and translation steps until convergence is attained. The coordinate system of the aligned map was subsequently resampled to the reference coordinate system using the chimera command 'vop'. Atomic coordinates of ribosomes obtained from the PDB were aligned to the reference model for the yeast 80S ribosome, based either on the small or large subunit rRNA, i.e. models based on crystal structures or cryo-EM reconstructions of the small subunits used the small subunit rRNA to align to the 18S rRNA (chain A) of PDB-1S1H, whereas models based on crystal structures or cryo-EM reconstructions of the large subunits used the large subunit rRNA to align to the 25S rRNA (chain 3) of PDB-1S1I. In contrast, models for the small and large subunit from crystal structures or cryo-EM reconstructions of 70S or 80S ribosomes were both aligned to the 25S rRNA (chain 3) of PDB-1S1I on the basis of the large subunit rRNA. This is necessary to retain the same relative orientation of the small and large subunit within the 70S or 80S ribosomes in the re-aligned positions. Since the atomic coordinates for the small and large subunit of a 70S or 80S ribosome are in separate PDB files due to their size, the alignment was done in two steps. Firstly, the large subunit was aligned as described above, and then the large subunit alignment matrix was applied to the small subunit. Alignment of the rRNA was performed by using the Matchmaker function in Chimera (31), which performs an initial pairwise alignment of the two rRNA sequences via the Needleman-Wunsch-Algorithm and the 'nucleic' substitution matrix, and then employs an iterative fit algorithm that removes aligned pairs until the root mean square deviation (RMSD) of the fitted pairs is <2Å.

LMU LUDWIG-MAXIMILIANS-UNIVERSITÄT MÜNCHEN **The DARC site**

All Search

Entry: 1858

Cryo-EM structure of the ribosome-SecYE complex in the membrane environment

EMDB file is associated with the following PDB models: 3j00, 3j01

Original file according to EMDB entry:
emd_1858.map.gz 8.47 MB

Aligned file:
emd_1858_aligned.brix 47.53 MB

Classification:
Bacteria

Organism:
Escherichia coli

Particle:
70S

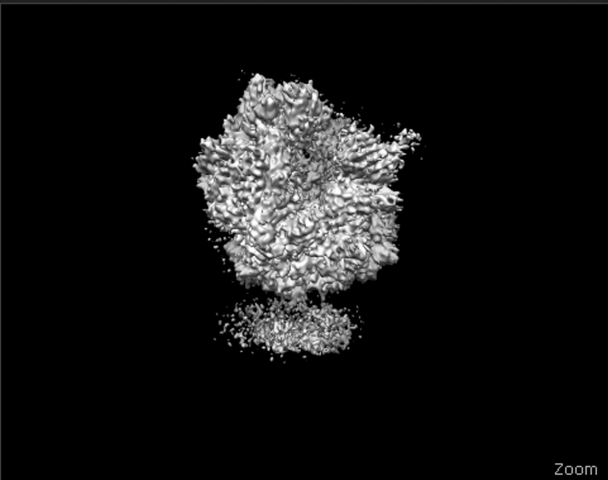
Ligand Name(s):
SecYEG

Method:
Cryo-EM

Publication authors:
Frauenfeld J, Gumbart J, van der Sluis EO, Funes S, Gartmann M, Beatrix B, Mielke T, Berninghausen O, Becker T, Schulten K, Beckmann R

Publication year:
2011

PubMed (ID: 21499241) citation:
The ubiquitous SecY-SecE1 complex translocates nascent secretory proteins across cellular membranes and integrates membrane proteins into lipid bilayers. Several structures of mostly detergent-solubilized Sec complexes have been reported. Here we present a single-particle cryo-EM structure of the SecYEG complex in a membrane environment, bound to a translating ribosome, at subnanometer resolution. Using the SecYEG complex reconstituted in a so-called Nanodisc, we could trace the nascent polypeptide chain from the peptidyltransferase center into the membrane. The reconstruction allowed for the identification of ribosome-lipid interactions. The rRNA helix 59 (H59) directly contacts the lipid surface and appears to modulate the membrane in immediate vicinity to the proposed lateral gate of the protein-conducting channel (PCC). On the basis of our map and molecular dynamics simulations, we present a model of a signal anchor-gated PCC in the membrane.



Zoom

Figure 1. Sample DARC output. Screen shot of DARC site output when searching for EMDB entry 1858.

Querying and retrieval from the DARC site

The DARC site has a user-friendly relational interface where users can either enter the known EMDB or PDB accession number (ID) into the search panel or use the drop-down menu to restrict the search to Source Database or ID (EMDB or PDB), title, author, abstract or PubMed ID, as well as method (cryo or X-ray), organism (chloroplast, *coli*, human, mitochondria, *thermophilus*, rabbit, *marismortui*), ligand (EF-G, EF2, SRP, tRNA, antibiotic), classification (bacteria, archaeon, eukaryote) or particle type (30S, 50S, 70S, 40S, 60S, 80S) (Figure 1). Search results are displayed as a list alphabetically arranged on the basis of the PDB or EMDB ID and the associated aligned DARC structures can be directly downloaded from the right-hand column by clicking the 'Aligned File' link.

Alternatively, the user can access further information on individual files by clicking the PDB or EMDB accession number link. An example of the retrieval of EMDB-1858 is shown in Figure 1. Each entry has a header with the title and a link to the original EMDB (or PDB file) is provided together with a link to the DARC aligned file, either as brix file for maps or pdb files for models. For EMDB entries having an associated PDB entry, additional links to the aligned files are provided below the title, for example, EMDB-1858 is associated with PDB entries 3J00 and 3J01. An automatically generated image of the relevant structure is presented on the right-hand side and additional details are presented on the left, including classification (e.g. bacteria), particle (70S), organism (e.g. *E. coli*), ligand name(s) (e.g. SecYEG), method (cryo-EM or X-ray),

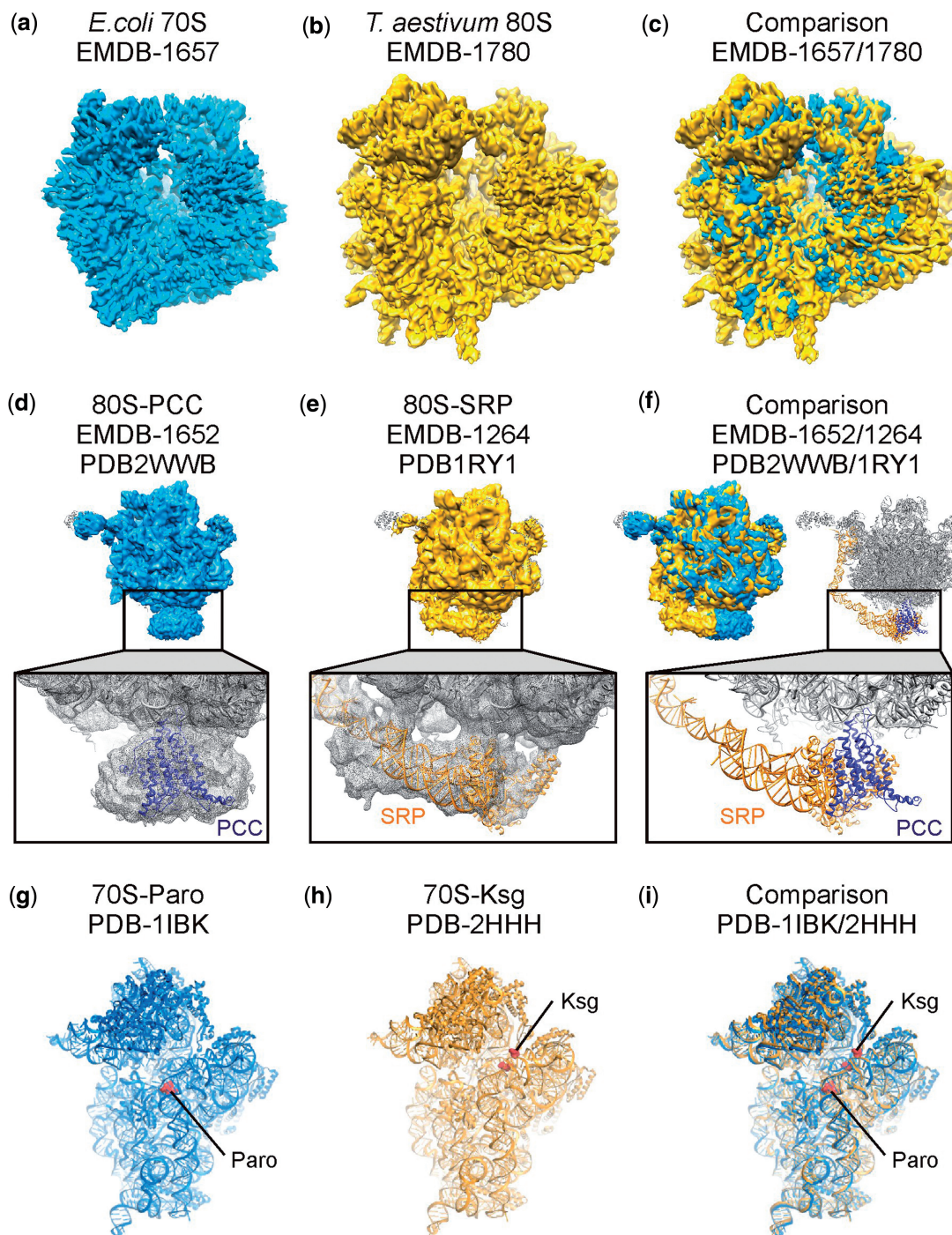


Figure 2. Example comparisons of DARC-aligned EMDB cryo-EM maps and PDB atomic coordinates. (a–c) Comparison of the cryo-EM map of the bacterial *E. coli* 70S ribosome (EMDB-1657) with the eukaryotic *T. aestivum* 80S ribosome (EMDB-1780). (d–f) Overview (above) and zoom (below) of the cryo-EM map and associated PDBs of the *T. aestivum* 80S ribosome bound with either the protein-conducting channel (PCC) (EMDB-1652/PDB-2WWB) or the signal recognition particle (SRP) (EMDB-1264/PDB-1RY1). (g–i) Comparison of the structures of the 30S subunit in complex with the antibiotic paromomycin (Paro) (PDB-1IBK) or kasugamycin (Ksg) (PDB-2HHH).

publication authors (Frauenfeld *et al.*), publication year (2011) and PubMed ID (with link to PubMed abstract).

Visualization of examples of DARC aligned maps and PDBs

Downloaded DARC-aligned map and pdb files can be opened in common viewers such as PyMol, Chimera (31)

or VMD (32) and directly compared. Figure 2a–c illustrates direct comparison of DARC aligned cryo-EM maps for a bacterial *E. coli* 70S ribosome (EMDB-1657) (34) with a eukaryotic *T. aestivum* 80S ribosome (EMDB-1780) (24,35). Alignment of cryo-EM maps and associated PDBs of the protein conducting channel (PCC) (36) and the signal recognition particle (SRP) (17) bound

to the *T. aestivum* 80S ribosome reveals an overlap in their binding site at the tunnel exit site (Figure 2d–f). Similarly, DARC-aligned PDBs comparing the antibiotic paromomycin [Paro; PDB-1IBK, (37)] and kasugamycin [Ksg; PDB-2HHH, (38)] bound to bacterial *T. thermophilus* 30S subunit reveal the different location of these drugs on the interface side of the particle (Figure 2g–i).

FUTURE PERSPECTIVES

Given the large number of crystal and NMR structures of ribosomal ligands determined in the non-bound state, one future perspective would be to incorporate these structures aligned to the ribosomal-bound form of the ligand. This would provide users with the ability to easily compare conformational changes that indeed occur in numerous ligands upon ribosome binding. Moreover, the database could be expanded progressively to include alignments of other large macromolecular complexes, that are subject to intense structural studies such as RNA polymerases (39) or AAA+ ATPases (40).

- Database name: The DARC site
- Main resource URL: <http://darcsite.genzentrum.lmu.de/darc/>
- Contact information (e-mail; postal mail): curator: hauser@lmb.uni-muenchen.de; Gene Center, Feodorlyenstr. 25, 81377 Munich, Germany
- Date resource established (year): 2011
- Conditions of use (Free, or type of license): Free
- Scope: data types captured, curation policy, standards used: PDB and brix files
- Standards: MIs, Data formats, terminologies: PDB and brix files
- Taxonomic coverage: All species
- Data accessibility/output options: download from URL
- Data release frequency: Updated monthly
- Versioning period and access to historical files: Yearly, None
- Documentation available: Not necessary
- User support options: Not necessary
- Data submission policy: Data parsed from PDB and EMDB
- Relevant publications: None
- Resource's Wikipedia URL: None
- Tools available: None

FUNDING

Deutsche Forschungsgemeinschaft SFB594 and SFB646 (to R.B.) and WI3285/1-1 (to D.N.W.). Funding for open access charge: Deutsche Forschungsgemeinschaft.

Conflict of interest statement. None declared.

REFERENCES

1. Schuwirth, B., Borovinskaya, M., Hau, C., Zhang, W., Vila-Sanjurjo, A., Holton, J., and Cate, J. (2005) Structures of the bacterial ribosome at 3.5 Å resolution. *Science*, **310**, 827–834.
2. Wimberly, B.T., Brodersen, D.E., Clemons, W.M., Morgan-Warren, R.J., Carter, A.P., Vonnrhein, C., Hartsch, T. and Ramakrishnan, V. (2000) Structure of the 30S ribosomal subunit. *Nature*, **407**, 327–339.
3. Schlueder, F., Tocilj, A., Zarivach, R., Harms, J., Gluehmann, M., Janell, D., Bashan, A., Bartels, H., Agmon, I., Franceschi, F. *et al.* (2000) Structure of functionally activated small ribosomal subunit at 3.3 Å resolution. *Cell*, **102**, 615–623.
4. Yusupov, M.M., Yusupova, G.Z., Baucom, A., Lieberman, K., Earnest, T.N., Cate, J.H. and Noller, H.F. (2001) Crystal structure of the ribosome at 5.5 Å resolution. *Science*, **292**, 883–896.
5. Selmer, M., Dunham, C., Murphy, F.t., Weixlbaumer, A., Petry, S., Kelley, A., Weir, J. and Ramakrishnan, V. (2006) Structure of the 70S ribosome complexed with mRNA and tRNA. *Science*, **313**, 1935–1942.
6. Harms, J., Schlueder, F., Zarivach, R., Bashan, A., Gat, S., Agmon, I., Bartels, H., Franceschi, F. and Yonath, A. (2001) High resolution structure of the large ribosomal subunit from a mesophilic eubacterium. *Cell*, **107**, 679–688.
7. Rabl, J., Leibundgut, M., Ataide, S.F., Haag, A. and Ban, N. (2010) Crystal structure of the eukaryotic 40S ribosomal subunit in complex with initiation factor 1. *Science*, **331**, 730–736.
8. Ben-Shem, A., Jenner, L., Yusupova, G. and Yusupov, M. (2010) Crystal structure of the eukaryotic ribosome. *Science*, **330**, 1203–1209.
9. Frank, J., Zhu, J., Penczek, P., Li, Y.H., Srivastava, S., Verschoor, A., Radermacher, M., Grassucci, R., Lata, R.K. and Agrawal, R.K. (1995) A model of protein synthesis based on cryo-electron microscopy of the *E. coli* ribosome. *Nature*, **376**, 441–444.
10. Connell, S.R., Takemoto, C., Wilson, D.N., Wang, H., Murayama, K., Terada, T., Shirouzu, M., Rost, M., Schuler, M., Giesebrecht, J. *et al.* (2007) Structural basis for interaction of the ribosome with the switch regions of GTP-bound elongation factors. *Mol. Cell*, **25**, 751–764.
11. Sharma, M.R., Wilson, D.N., Datta, P.P., Barat, C., Schlueder, F., Fucini, P. and Agrawal, R.K. (2007) Cryo-EM study of the spinach chloroplast ribosome reveals the structural and functional roles of plastid-specific ribosomal proteins. *Proc. Natl Acad. Sci. USA*, **104**, 19315–19320.
12. Sharma, M.R., Koc, E.C., Datta, P.P., Booth, T.M., Spremulli, L.L. and Agrawal, R.K. (2003) Structure of the mammalian mitochondrial ribosome reveals an expanded functional role for its component proteins. *Cell*, **115**, 97–108.
13. Spahn, C.M., Kieft, J.S., Grassucci, R.A., Penczek, P.A., Zhou, K., Doudna, J.A. and Frank, J. (2001) Hepatitis C virus IRES RNA-induced changes in the conformation of the 40s ribosomal subunit. *Science*, **291**, 1959–1962.
14. Dube, P., Wieske, M., Stark, H., Schatz, M., Stahl, J., Zemlin, F., Lutsch, G. and van Heel, M. (1998) The 80S rat liver ribosome at 25 Å resolution by electron cryomicroscopy and angular reconstruction. *Structure*, **6**, 389–399.
15. Dube, P., Bacher, G., Stark, H., Mueller, F., Zemlin, F., van Heel, M. and Brimacombe, R. (1998) Correlation of the expansion segments in mammalian rRNA with the fine structure of the 80 S ribosome; a cryoelectron microscopic reconstruction of the rabbit reticulocyte ribosome at 21 Å resolution. *J. Mol. Biol.*, **279**, 403–421.
16. Chandramouli, P., Topf, M., Menetret, J.F., Eswar, N., Cannone, J.J., Gutell, R.R., Sali, A. and Akey, C.W. (2008) Structure of the mammalian 80S ribosome at 8.7 Å resolution. *Structure*, **16**, 535–548.
17. Halic, M., Becker, T., Pool, M., Spahn, C., Grassucci, R., Frank, J. and Beckmann, R. (2004) Structure of the signal recognition particle interacting with the elongation-arrested ribosome. *Nature*, **427**, 808–814.
18. Spahn, C.M., Beckmann, R., Eswar, N., Penczek, P.A., Sali, A., Blobel, G. and Frank, J. (2001) Structure of the 80S ribosome from *Saccharomyces cerevisiae*-tRNA-ribosome and subunit-subunit interactions. *Cell*, **107**, 373–386.
19. Sengupta, J., Nilsson, J., Gursky, R., Spahn, C., Nissen, P. and Frank, J. (2004) Identification of the versatile scaffold protein RACK1 on the eukaryotic ribosome by cryo-EM. *Nat. Struct. Mol. Biol.*, **11**, 957–962.

20. Dutta,S., Burkhardt,K., Young,J., Swaminathan,G.J., Matsuura,T., Henrick,K., Nakamura,H. and Berman,H.M. (2009) Data deposition and annotation at the worldwide protein data bank. *Mol. Biotechnol.*, **42**, 1–13.
21. Lawson,C.L., Baker,M.L., Best,C., Bi,C., Dougherty,M., Feng,P., van Ginkel,G., Devkota,B., Lagerstedt,I., Ludtke,S.J. *et al.* (2011) EMDataBank.org: unified data resource for CryoEM. *Nucleic Acids Res.*, **39**, D456–D464.
22. Schmeing,T.M. and Ramakrishnan,V. (2009) What recent ribosome structures have revealed about the mechanism of translation. *Nature*, **461**, 1234–1242.
23. Klein,D., Moore,P. and Steitz,T. (2004) The roles of ribosomal proteins in the structure assembly, and evolution of the large ribosomal subunit. *J. Mol. Biol.*, **340**, 141–177.
24. Armache,J.P., Jarasch,A., Anger,A.M., Villa,E., Becker,T., Bhushan,S., Jossinet,F., Habeck,M., Dindar,G., Franckenberg,S. *et al.* (2010) Cryo-EM structure and rRNA model of a translating eukaryotic 80S ribosome at 5.5-Å resolution. *Proc. Natl Acad. Sci. USA*, **107**, 19748–19753.
25. Frank,J. and Agrawal,R.K. (2000) A ratchet-like inter-subunit reorganization of the ribosome during translocation. *Nature*, **406**, 318–322.
26. Dunkle,J.A., Wang,L., Feldman,M.B., Pulk,A., Chen,V.B., Kapral,G.J., Noeske,J., Richardson,J.S., Blanchard,S.C. and Cate,J.H. (2011) Structures of the bacterial ribosome in classical and hybrid states of tRNA binding. *Science*, **332**, 981–984.
27. Wilson,D.N., Harms,J.M., Nierhaus,K.H., Schlünzen,F. and Fucini,P. (2005) Species-specific antibiotic-ribosome interactions: Implications for drug development. *Biol. Chem.*, **386**, 1239–1252.
28. Simonovic,M. and Steitz,T.A. (2009) A structural view on the mechanism of the ribosome-catalyzed peptide bond formation. *Biochim. Biophys. Acta*, **1789**, 612–623.
29. Fischer,N., Konevega,A.L., Wintermeyer,W., Rodnina,M.V. and Stark,H. (2010) Ribosome dynamics and tRNA movement by time-resolved electron cryomicroscopy. *Nature*, **466**, 329–333.
30. Ratje,A.H., Loerke,J., Mikolajka,A., Brunner,M., Hildebrand,P.W., Starosta,A.L., Donhofer,A., Connell,S.R., Fucini,P., Mielke,T. *et al.* (2010) Head swivel on the ribosome facilitates translocation by means of intra-subunit tRNA hybrid sites. *Nature*, **468**, 713–716.
31. Pettersen,E.F., Goddard,T.D., Huang,C.C., Couch,G.S., Greenblatt,D.M., Meng,E.C. and Ferrin,T.E. (2004) UCSF Chimera - A Visualization System for Exploratory Research and Analysis. *J. Comput. Chem.*, **25**, 1605–1612.
32. Humphrey,W., Dalke,A. and Schulten,K. (1996) VMD - visual molecular dynamics. *J. Mol. Graphics*, **14**, 33–38.
33. Frank,J., Radermacher,M., Penczek,P., Zhu,J., Li,Y., Ladjadj,M. and Leith,A. (1996) SPIDER and WEB: processing and visualization of images in 3D electron microscopy and related fields. *J. Struct. Biol.*, **116**, 190–199.
34. Seidelt,B., Innis,C.A., Wilson,D.N., Gartmann,M., Armache,J.P., Villa,E., Trabuco,L.G., Becker,T., Mielke,T., Schulten,K. *et al.* (2009) Structural insight into nascent polypeptide chain-mediated translational stalling. *Science*, **326**, 1412–1415.
35. Armache,J.P., Jarasch,A., Anger,A.M., Villa,E., Becker,T., Bhushan,S., Jossinet,F., Habeck,M., Dindar,G., Franckenberg,S. *et al.* (2010) Localization of eukaryote-specific ribosomal proteins in a 5.5-Å cryo-EM map of the 80S eukaryotic ribosome. *Proc. Natl Acad. Sci. USA*, **107**, 19754–19759.
36. Becker,T., Bhushan,S., Jarasch,A., Armache,J.P., Funes,S., Jossinet,F., Gumbart,J., Mielke,T., Berninghausen,O., Schulten,K. *et al.* (2009) Structure of monomeric yeast and mammalian Sec61 complexes interacting with the translating ribosome. *Science*, **326**, 1369–1373.
37. Ogle,J.M., Brodersen,D.E., Clemons,W.M. Jr, Tarry,M.J., Carter,A.P. and Ramakrishnan,V. (2001) Recognition of cognate transfer RNA by the 30S ribosomal subunit. *Science*, **292**, 897–902.
38. Schluzen,F., Takemoto,C., Wilson,D.N., Kaminishi,T., Harms,J.M., Hanawa-Suetsugu,K., Szaflarski,W., Kawazoe,M., Shirouzu,M., Nierhaus,K.H. *et al.* (2006) The antibiotic kasugamycin mimics mRNA nucleotides to destabilize tRNA binding and inhibit canonical translation initiation. *Nat. Struct. Mol. Biol.*, **13**, 871–878.
39. Cramer,P., Armache,K.J., Baumli,S., Benkert,S., Brueckner,F., Buchen,C., Damsma,G.E., Dengl,S., Geiger,S.R., Jasiak,A.J. *et al.* (2008) Structure of eukaryotic RNA polymerases. *Annu. Rev. Biophys.*, **37**, 337–352.
40. Saibil,H.R. (2008) Chaperone machines in action. *Curr. Opin. Struct. Biol.*, **18**, 35–42.